Electrospun Self-Standing Membrane of Hierarchical SiO₂@γ-AlOOH (Boehmite) Core/Sheath Fibers for Water Remediation

Yue-E Miao, Ruiyu Wang, Dan Chen, Zhenyan Liu, and Tianxi Liu*

State Key Laboratory of Molecular Engineering of Polymers, Department of Macromolecular Science, Fudan University, Shanghai 200433, People's Republic of China

ABSTRACT: Hierarchical SiO₂@γ-AlOOH (Boehmite) core/sheath fibers are fabricated based on a combination of electrospinning and hydrothermal reaction. γ-AlOOH (Boehmite) nanoplatelets are uniformly anchored on the surface of SiO₂ fibers, which significantly improves the adsorption efficiency of the SiO₂ fiber membrane for organic dyes and microorganisms. Compared to conventional nanoparticle adsorbents, the self-standing membrane thus prepared is highly flexible and easy to handle and retrieve, making it a promising material for water treatment. By virtue of electrospinning and a hydrothermal reaction, it provides possibilities to fabricate other functional fiber membranes with hierarchical structures, which can find potential applications in adsorption, catalysis, filtration, and other environmental remediation fields.

KEYWORDS: electrospinning, self-standing membrane, hierarchical structure, water remediation
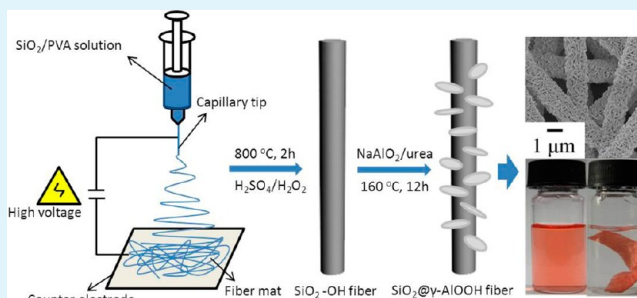
1. INTRODUCTION

Environmental problems of organic and toxic waste in water pose a major health risk to humankind. Contamination of water with organic dyes (e.g., Congo red, methylene blue and malachite green), heavy-metal ions (e.g., Pb^{2+}, Cr^{3+}, and Cd^{2+}), and microorganisms (e.g., *Escherichia coli*, *Staphylococcus aureus*, and *Sarcina lutea*) is becoming a severe environmental and public health problem; thereby water purification technology has attracted much attention recently.[1,2] As an effective approach, adsorption has been extensively employed for water treatment, where a variety of advanced materials have been studied as adsorbents, such as porous carbons,[3,4] mesoporous silicas,[5,6] and other hierarchical materials.[7,8] γ-AlOOH (Boehmite) is an aluminum oxyhydroxide, which is the precursor of γ-Al_2O_3 and is usually used as catalyst supports, adsorbents, and ceramics. Thus far, various hierarchically structured Boehmite, such as nanoplatelets, nanofibers, nanotubes, hollow microspheres, and flowerlike three-dimensional (3D) nanoarchitectures, have been prepared successfully.[9–12] Exhibiting an AlO_6 octahedral lamellar structure with plenty of OH groups on the surface, Boehmite is inclined to interact with foreign molecules or heavy-metal ions, which makes it an excellent candidate for water decontamination.[13,14] Nevertheless, because of their superior dispersive properties, nanoparticles (NPs) with small dimensions are difficult to recycle by conventional separation methods including centrifugation or filtration. Worse still, it may lead to loss of the adsorbent and bring about secondary pollution to the environment.[15,16] Therefore, the development of new adsorbents having large surface area, high adsorption efficiency, and

easy retrieval properties is considered to be of significant importance in practical environmental engineering applications.

Electrospinning is a promising and straightforward technique that produces continuous fibers with diameters in the range of nanometers to a few micrometers. These fibers possess high surface area to volume ratios, high porosities, and other outstanding properties, making them excellent candidates for sensors, catalysts, and ultrafiltration and separation membranes.[17–19] Therefore, electrospun fibrous membranes have been widely used as matrixes or templates to fabricate various hierarchical nanostructures for remediation and pollution control applications.[20–22] Lee et al. have used a layer-by-layer deposition approach to immobilize TiO_2 NPs on a porous electrospun polymer fiber mesh with high surface area, which leads to a stable structure and improved photocatalytic activities for long-term photochemical water remediation.[23] Fang et al. have employed water-insoluble electrospun polyethylenimine (PEI)/poly(vinyl alcohol) (PVA) nanofibers as nanoreactors to bind $AuCl^{4-}$ anions via the free amine groups of PEI first, which was followed by the in situ reduction of $AuCl^{4-}$ anions to form gold NPs (AuNPs).[24] Other kinds of metal NPs (e.g., palladium and zerovalent iron) also have been immobilized on the surface of electrospun nanofibers for efficient removal of pollutant dyes and heavy-metal ions.[25,26] Caruso et al. and Hyuk et al. have combined electrospinning and the sol–gel process to achieve metal oxide precursor nanocoating, which was followed by calcination to obtain metal oxide nanotubes for
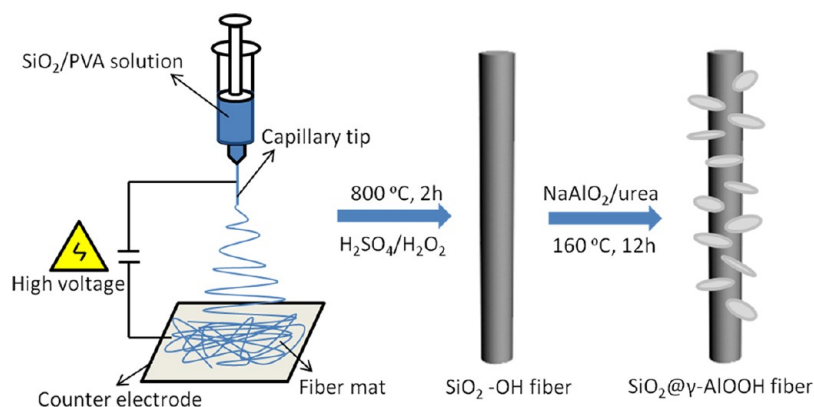
Figure 1. Schematic illustration of the preparation of SiO$_2$@γ-AlOOH (Boehmite) core/sheath fibers.

adsorption and photocatalytic decomposition of Rhodamine B.[27,28] In our previous study,[29] a flexible electrospun membrane of ZnO/SiO$_2$ hierarchical structure has also been developed by the hydrothermal epitaxial growth of ZnO nanorods on the surface of SiO$_2$ fibers, which exhibited excellent photocatalytic efficiency and recycling ability toward organic dyes.

Recently, surface coating or modification has received significant attention because of its diversity to build complex micro/nanostructures.[29,30] SiO$_2$ with activated OH groups has been widely used in coating treatments. Because of its high flexibility and thermal stability, an electrospun SiO$_2$ fiber membrane is considered to be the ideal matrix for further construction of hierarchical structures through hydrothermal treatment,[29] in situ polymerization,[31] and traditional physical vapor deposition.[32] Herein, we report the preparation of a self-standing membrane of hierarchical SiO$_2$@γ-AlOOH (Boehmite) core/sheath fibers through the hydrothermal growth of Boehmite on the surface of electrospun SiO$_2$ fibers. The membrane thus obtained possesses an open structure, which is propitious for direct interaction between the adsorbent and pollutants or bacteria. The adsorption performance of SiO$_2$ and SiO$_2$@γ-AlOOH (Boehmite) core/sheath fiber membranes toward the organic dye and bacteria shows that the organic dye and bacteria removal efficiency is significantly enhanced after anchoring Boehmite on the surface of SiO$_2$ fibers. Moreover, the adsorbent in flexible membrane form can be easily manipulated and retrieved, which further broadens its potential applications in water remediation fields.

2. EXPERIMENTAL SECTION

Materials. Poly(vinyl alcohol) (PVA; M_w from 85000 to 124000 g/mol, Sigma) and tetraethyl orthosilicate (TEOS; Lingfeng Chemical Co., Ltd., China) were used. *S. aureus* was obtained from American Type Culture Collection. Phosphate-buffered saline (PBS; pH = 7.0) was prepared from analytical-grade chemicals. All other reagents of analytical grade were commercially available from Sinopharm Chemical Reagent Co., Ltd., and used without further purification.

Preparation of Electrospun SiO$_2$ Fibers. The electrospun SiO$_2$ fibers were produced according to the literature.[33] A silica gel with a molar composition of TEOS:H$_3$PO$_4$:H$_2$O = 1:0.01:11 was prepared through hydrolysis and polycondensation. Then, an equivalent weight of 10 wt % PVA aqueous solution was dropped slowly into the silica gel to improve the electrospinnability. The mixture was vigorously stirred at room temperature until a viscous solution of the PVA/SiO$_2$ composite was obtained. After that, the solution was transferred into a plastic syringe for electrospinning at a fixed electrical potential of 16 kV. The electrospinning solution was fed at a speed of 1.0 mL/h with a distance of 20 cm between the needle tip and collector. The fiber

membrane was collected on aluminum foil and then peeled off to be calcined at 800 °C in air for 2 h to remove PVA. Thus, a pure SiO$_2$ fibrous membrane was obtained for further experiments.

Preparation of SiO$_2$@γ-AlOOH (Boehmite) Core/Sheath Fibers. The synthesis process of SiO$_2$@γ-AlOOH (Boehmite) core/sheath fibers is described briefly as follows. The as-prepared SiO$_2$ fiber membrane was first immersed in a bath of H$_2$SO$_4$/H$_2$O$_2$ (3:1, v/v) for about 1 h and thoroughly rinsed with deionized water. Then, the membrane was hydrothermally treated in a stainless steel autoclave containing a 35 mL solution of sodium aluminate (NaAlO$_2$; 10.2 g/L) and urea (NH$_2$CONH$_2$; 28.8 g/L) at 160 °C for 12 h. After cooling to room temperature, the sample was rinsed with deionized water several times and dried in a vacuum oven at 50 °C for 6 h. The content of Boehmite in a SiO$_2$@γ-AlOOH (Boehmite) core/sheath fiber membrane was calculated from the mass difference of the membrane before and after hydrothermal treatment. The whole preparation procedure of a SiO$_2$@γ-AlOOH (Boehmite) core/sheath fiber membrane is schematically shown in Figure 1.

Characterization. X-ray diffraction (XRD) patterns of the samples were conducted from $2\theta = 10°$ to $80°$ on an X'Pert Pro X-ray diffractometer with Cu Kα radiation ($\lambda = 0.1542$ nm) under a voltage of 40 kV and a current of 40 mA. The morphology and fiber diameters of the samples were investigated using a scanning electron microscope (Tescan) at an acceleration voltage of 20 kV. Both SiO$_2$ and SiO$_2$@γ-AlOOH (Boehmite) core/sheath fiber membranes were gold sputter-coated prior to scanning electron microscopy (SEM) observations.

Measurements of the Adsorption Performance. Adsorption measurements for Congo red were performed by adding a SiO$_2$ or SiO$_2$@γ-AlOOH (Boehmite) core/sheath fiber membrane with dimensions of 1.5 cm × 0.5 cm into 3 mL of a Congo red solution (50 mg/L). At selected time intervals, the Congo red solution was measured for Congo red concentrations at 500 nm using a Perkin-Elmer Lambda 35 UV–vis absorption spectrophotometer. The calibration curve of Congo red was prepared by measuring the absorbances of different predetermined concentrations of the sample. The adsorption performance of Congo red on Boehmite powder was also carried out as a reference sample.

Evaluation of the *S. aureus* adhesive properties on these fiber membranes was performed by direct SEM observations. Briefly, SiO$_2$ and SiO$_2$@γ-AlOOH (Boehmite) core/sheath fiber membranes were first incubated in a 1.0 mL suspension of *S. aureus* (10^9 cells/mL) for 24 h, respectively. Then, the membranes were washed three times with PBS for removal of the nonadhered bacteria. Afterward, the nanofibrous membranes were incubated in 3% glutaraldehyde at 4 °C for 5 h. Finally, the membranes were taken out and washed with PBS, followed by step dehydration with 25%, 50%, 70%, 95%, and 100% ethanol for 10 min each. The membranes were finally dried under vacuum and gold sputter-coated prior to SEM observations.

The surface spread plate method was performed to further evaluate the adhesive properties of bacteria on the fiber membranes. The membranes were first washed with 75% ethanol to kill any bacteria on their surfaces and then respectively immersed in 1 mL of the bacterial

suspension at 37 °C. After 24 h of incubation, the membranes were removed from the bacterial suspension with sterile forceps and gently washed twice with PBS. The bacteria retained on the membranes were dislodged in 1 mL of PBS for 10 min by mild ultrasonication. Finally, the viable cell counts of bacteria on the membranes were measured by the surface spread plate method.

3. RESULTS AND DISCUSSION

Structure and Morphology of SiO$_2$@γ-AlOOH (Boehmite) Core/Sheath Fibers. XRD was used to monitor the
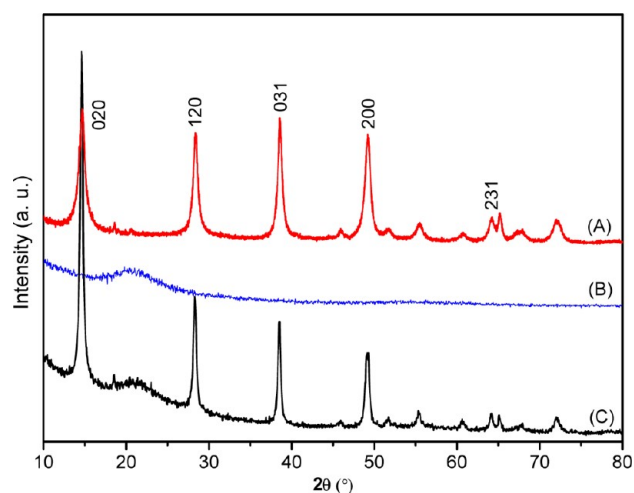

Figure 2. XRD patterns of (A) Boehmite particles, (B) SiO$_2$ fibers, and (C) SiO$_2$@γ-AlOOH (Boehmite) core/sheath fibers.

structure of the as-prepared products (Figure 2). In the XRD pattern of the obtained Boehmite particles (curve A), five
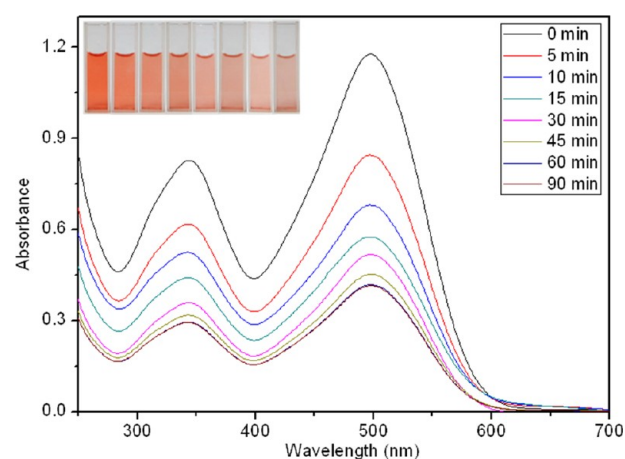

Figure 4. Absorption spectra of Congo red in the presence of a SiO$_2$@γ-AlOOH (Boehmite) core/sheath fiber membrane after time intervals of 0, 5, 10, 15, 30, 45, 60, and 90 min. The insets are the corresponding digital photographs of Congo red solutions at the same time when the UV−vis spectra are taken.

typical peaks at 14.2°, 27.8°, 38.3°, 49.1°, and 64.1° are observed, which represent the (020), (120), (031), (200), and (231) reflections of orthorhombic Boehmite, respectively. Only a broad halo is observed in curve B, indicating an amorphous structure of electrospun SiO$_2$ fibers. In comparison to SiO$_2$ fibers, basal peaks of the inorganic component are clearly seen in the XRD pattern of SiO$_2$@γ-AlOOH (Boehmite) core/sheath fibers (curve C), showing the successful immobilization of Boehmite on the surface of SiO$_2$ fibers.

The morphology and fiber diameters of SiO$_2$ and SiO$_2$@γ-AlOOH (Boehmite) core/sheath fibers were investigated by
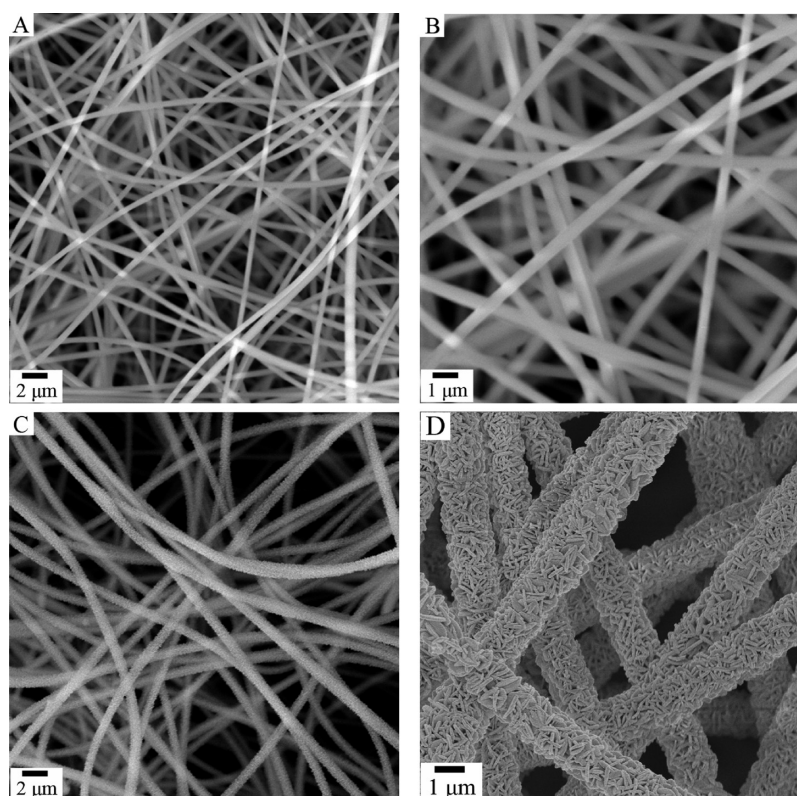

Figure 3. Low- and high-magnification SEM images of (A and B) SiO$_2$ fibers and (C and D) SiO$_2$@γ-AlOOH (Boehmite) core/sheath fibers.
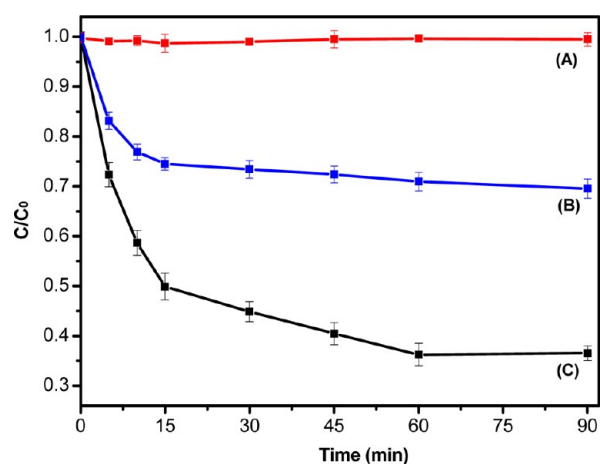
Figure 5. Adsorption rates of Congo red on (A) SiO$_2$ fiber membrane, (B) Boehmite powder, and (C) SiO$_2$@γ-AlOOH (Boehmite) core/sheath fiber membrane, respectively.

Figure 7. (A) Digital picture of the self-standing SiO$_2$@γ-AlOOH (Boehmite) core/sheath fiber membrane and (B) digital pictures of a Congo red solution before (a) and after (b) adsorption by a SiO$_2$@γ-AlOOH (Boehmite) core/sheath fiber membrane for over 90 min.
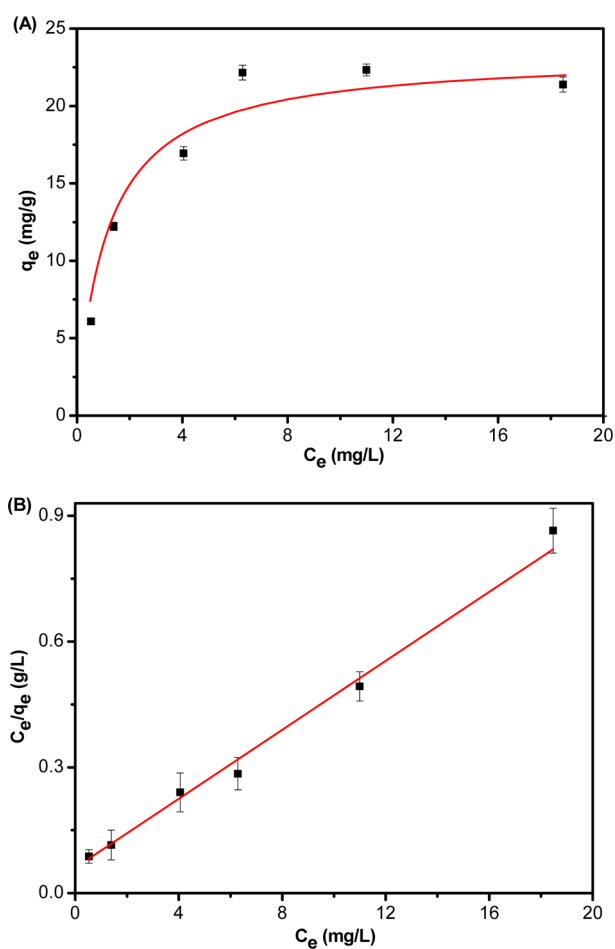

Figure 6. (A) Adsorption isotherms and (B) corresponding Langmuir plots of Congo red on SiO$_2$@γ-AlOOH (Boehmite) core/sheath fiber membranes for over 90 min.

SEM, as shown in Figure 3. SiO$_2$ fibers were obtained through the sol−gel method, which was followed by the removal of PVA via calcination. Because of their high flexibility and thermal stability, electrospun SiO$_2$ fibers were selected as the matrix to further construct the hierarchical structure. The average diameter of SiO$_2$ fibers is about 500 nm (Figure 3A,B), while
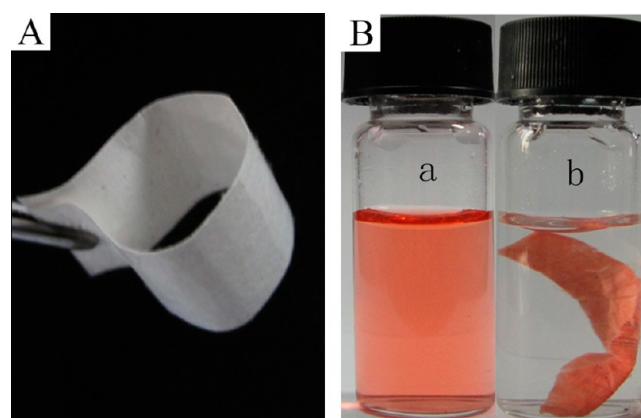
the diameter of SiO$_2$@γ-AlOOH (Boehmite) core/sheath fibers increases to about 1.2 μm (Figure 3C,D). This indicates that the average size of Boehmite NPs anchored on the fiber surface is about 350 nm. Close observation of the SiO$_2$@γ-AlOOH (Boehmite) core/sheath fibers (Figure 3D) reveals that all of the Boehmite nanoplatelets are grown perpendicular to the surface of the SiO$_2$ fibers. Thus, a hierarchical 3D structure is constructed through a well-controlled combination of one-dimensional (1D) nanofibers and two-dimensional (2D) nanoplatelets, forming well-structured core/sheath fibers. Compared to the cases when NPs are fixed in the fibrous membrane, this open structure offers a much higher contact area between the adsorbent and water solution, which can be a vital factor in determining the adsorption efficiency.

Adsorption Performance in Water Remediation. The above self-standing membrane of SiO$_2$@γ-AlOOH (Boehmite) core/sheath fibers was used as the adsorbent for potential applications in water remediation because of its unique hierarchical porous structure. Congo red, a common azo dye in the textile industry, was selected as a typical pollutant in water resources. UV−vis absorption spectroscopy measurements were performed to determine the dye concentrations before and after adsorption by a SiO$_2$@γ-AlOOH (Boehmite) core/sheath fiber membrane at selected time intervals, as shown in Figure 4. The obvious decrease in the absorption peaks indicates an efficient adsorption of Congo red on the membrane. Digital pictures (the inset in Figure 4) were taken at the same selected time intervals to visually depict the whole adsorption process. The characteristic absorption of Congo red around 500 nm was chosen to illustrate the adsorption performance quantitatively. C/C_0 was used to characterize the relative adsorption capacity (C_0 and C represent the initial concentration of Congo red and its concentration after adsorption, respectively). A comparative study was carried out under the same experimental conditions for adsorption of Congo red using Boehmite powder and a SiO$_2$ fiber membrane. As can be seen from Figure 5, a SiO$_2$ fiber membrane almost has no adsorption for Congo red even after an equilibrium time of 90 min, whereas Congo red was immediately adsorbed on a SiO$_2$@γ-AlOOH (Boehmite) core/sheath fiber membrane within 15 min ($C/C_0 = 0.50$). Moreover, the adsorption of Congo red almost reached equilibrium only after 60 min ($C/C_0 = 0.36$) with a saturation adsorption capacity of 6.4 mg/g.
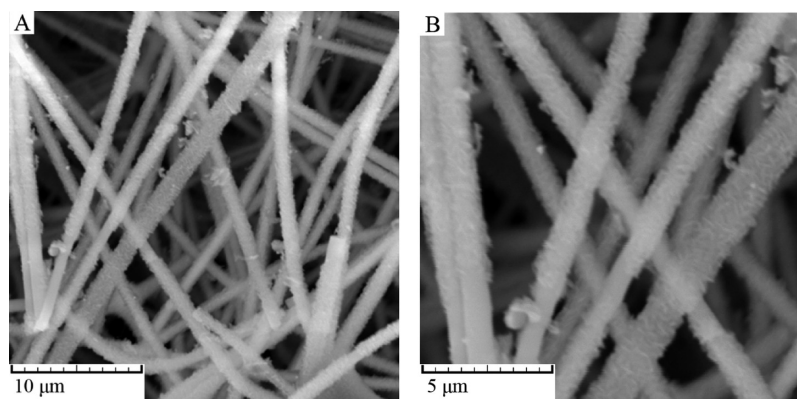
Figure 8. (A) Low- and (B) high-magnification SEM images of a SiO₂@γ-AlOOH core/sheath fiber membrane after adsorption in a Congo red solution for over 90 min.
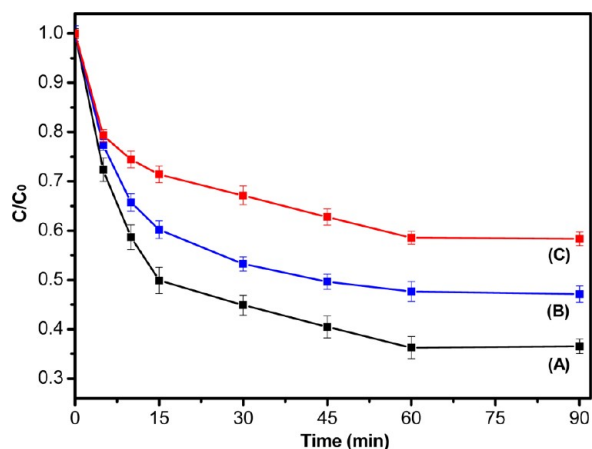

Figure 9. Adsorption rates of Congo red on a SiO₂@γ-AlOOH (Boehmite) core/sheath fiber membrane after the (A) first, (B) second, and (C) third cycles.

Thus, it can be seen that the removal of Congo red is mainly due to the Boehmite nanoplatelets that are anchored on the surface of SiO₂ fibers. According to a previous study,[34] the adsorption between Congo red and Boehmite happens through electrostatic attraction and hydrogen bonding between the hydroxyl groups present on the surface of Boehmite and the amine groups of Congo red molecules. Because the loading content of Boehmite nanoplatelets in a SiO₂@γ-AlOOH (Boehmite) core/sheath fiber membrane is 30 wt %, the saturation adsorption capacity of Congo red on Boehmite nanoplatelets is calculated as 21.3 mg/g. For comparison, the adsorption efficiency of Congo red using the same amount of Boehmite powder as the adsorbent was also tested. From Figure 5B, it can be seen that the adsorption rate of Congo red on Boehmite powder is only half that of a SiO₂@γ-AlOOH (Boehmite) core/sheath fiber membrane, with a saturation adsorption capacity of 10.4 mg/g after 90 min ($C/C_0 = 0.70$). Furthermore, the adsorption capacity of the organic dye on a SiO₂@γ-AlOOH (Boehmite) core/sheath fiber membrane is higher than that of other adsorbents previously reported, such as free-standing alumina nanofiber thin films (1.80 mg/g), electrospun mesoporous TiO₂ fibers (19.03 mg/g), and hierarchical films of layered double hydroxides (20 mg/g).[35−37] These results thus indicate that the hierarchical porous structure of SiO₂@γ-AlOOH (Boehmite) core/sheath fibers can be beneficial for enhancing the adsorption efficiency. First,

the distribution of Boehmite nanoplatelets can obviously be improved after their anchoring on the surface of SiO₂ fibers. Then, the hierarchical porous structure offers a much higher contact area between the adsorbent and water solution, which greatly facilitates diffusion of the relatively large organic dye molecules.

The adsorption isotherm was performed to further illustrate the adsorption process of Congo red on the hierarchical SiO₂@γ-AlOOH (Boehmite) core/sheath fiber membrane, as shown in Figure 6A. The Langmuir adsorption isotherm, eq 1,[38] was chosen to fit the adsorption isotherm:

$$C_e/q_e = 1/(q_m K_L) + C_e/q_m \tag{1}$$

where C_e (mg/L), q_e (mg/g), q_m (mg/g), and K_L (L/mg) are the equilibrium solute concentration, equilibrium adsorption capacity, maximum adsorption capacity, and adsorption constant, respectively. The regression equation was shown as follows: $C_e/q_e = 0.0604 + 0.0412C_e$ with the square of the correlation coefficient of 0.991 for the SiO₂@γ-AlOOH (Boehmite) core/sheath fiber membrane (Figure 6B), indicating that the adsorption of Boehmite for Congo red still fits well to the Langmuir model after being immobilized on the surface of SiO₂ fibers. The maximum adsorption capacity of Congo red on Boehmite nanoplatelets in a SiO₂@γ-AlOOH (Boehmite) core/sheath fiber membrane is found to be 24.3 mg/g.

Figure 7A shows the digital picture of the self-standing SiO₂@γ-AlOOH (Boehmite) core/sheath fiber membrane. No crack appears upon bending, indicating high flexibility of the fiber membrane, which may be due to the small size of the fibers.[30] The adsorbent in flexible membrane form (Figure 7B) can be manipulated and separated more conveniently than that in the powdery form. After adsorption in a Congo red solution for over 90 min, the SiO₂@γ-AlOOH (Boehmite) core/sheath fiber membrane was further observed by SEM (Figure 8). The hierarchical structure of the SiO₂@γ-AlOOH (Boehmite) core/sheath fiber membrane is almost intact, with γ-AlOOH nanoplatelets well-adhered on the fiber surface. Furthermore, a SiO₂@γ-AlOOH (Boehmite) core/sheath fiber membrane could be regenerated by simple thermal treatment in air at 280 °C. From Figure 9, it can be seen that the final adsorption capacity of Congo red on the membrane after three cycles is still higher than that of Boehmite powder. The reduction of the adsorption performance during the cyclic test can be attributed to the decrease of OH groups on the surface of Boehmite nanoplatelets after heat treatment. In general, the self-standing membrane of hierarchical SiO₂@γ-AlOOH (Boehmite) core/
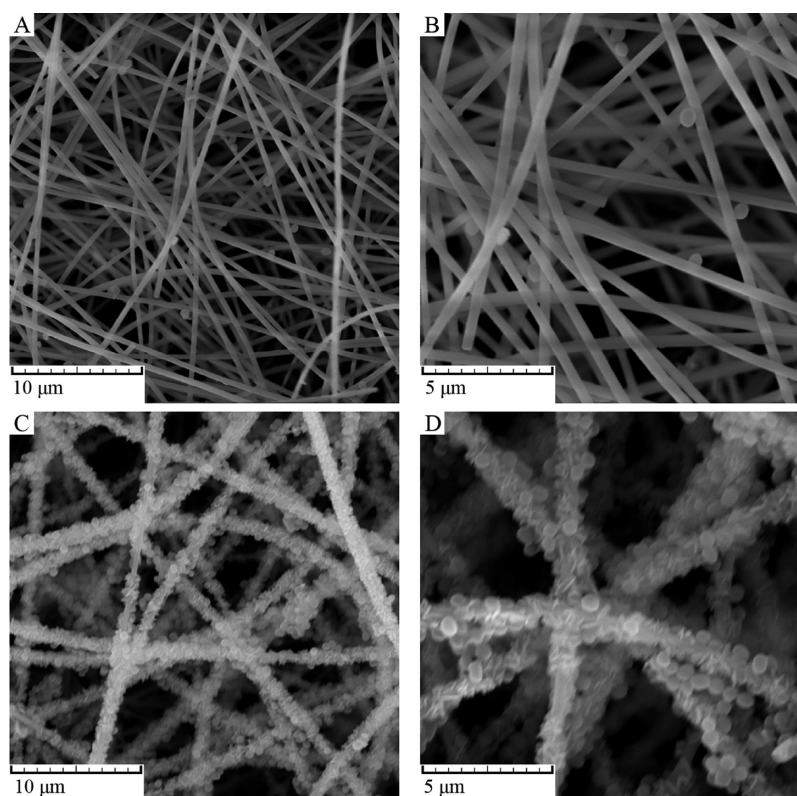
Figure 10. SEM images of (A) SiO$_2$ and (B) SiO$_2$@γ-AlOOH (Boehmite) core/sheath fiber membranes after *S. aureus* adhesion.

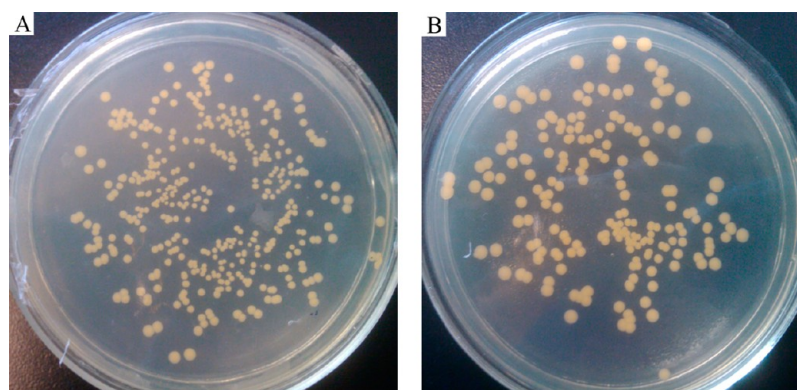**Figure 11.** Photographs of the viable cells (colonies) dislodged from (A) SiO$_2$ and (B) SiO$_2$@γ-AlOOH (Boehmite) core/sheath fiber membranes in the surface spread plate method.

sheath fibers could be an excellent adsorbent for organic dyes in water treatment.

The ability of SiO$_2$ and SiO$_2$@γ-AlOOH (Boehmite) core/sheath fiber membranes to capture bacterial pathogens was examined using the Gram-positive bacteria *S. aureus* as a model microorganism. Figure 10 shows the capture efficiency of *S. aureus* on SiO$_2$ and SiO$_2$@γ-AlOOH (Boehmite) core/sheath fiber membranes after 24 h of incubation. It can be seen that few bacterial pathogens are trapped by SiO$_2$ fibers (Figure 10A,B), while the capture efficiency significantly increases on SiO$_2$@γ-AlOOH (Boehmite) core/sheath fiber membrane (Figure 10C,D). The adhesive activities of *S. aureus* on the fiber membranes are further assessed by the surface spread plate method, as shown in Figure 11. The viable cell (colony) counts of bacteria dislodged from SiO$_2$ and SiO$_2$@γ-AlOOH (Boehmite) core/sheath fiber membranes by ultrasonication

are 394×10^5 and 193×10^5 cells/cm^2, respectively. That is to say, the cell number dislodged from a SiO$_2$ fiber membrane is much larger than that from a SiO$_2$@γ-AlOOH (Boehmite) core/sheath fiber membrane, whereas the capture efficiency of bacteria on a SiO$_2$@γ-AlOOH (Boehmite) core/sheath fiber membrane is significantly higher than that on a SiO$_2$ fiber membrane, according to the SEM images in Figure 10. Thus, it can be inferred that the adhesion of bacteria on SiO$_2$@γ-AlOOH (Boehmite) core/sheath fiber membrane is much stronger than that on a SiO$_2$ fiber membrane under the same ultrasonication conditions, which makes it promising in the removal of bacterial pathogens from water.

4. CONCLUSIONS

In summary, SiO$_2$@γ-AlOOH (Boehmite) core/sheath fibers have successfully been fabricated through a combination of

electrospinning and hydrothermal treatment. The hierarchical structure of Boehmite on SiO_2 fibers obviously improves the distribution of Boehmite nanoplatelets and offers a direct contact area between Boehmite and a water solution, which facilitates diffusion and adsorption of the relatively large organic dye molecules and microorganisms. Because of the high flexibility and easy retrieval properties of the self-standing $SiO_2@\gamma$-AlOOH (Boehmite) core/sheath fiber membrane, this approach provides possibilities for the facile construction and fabrication of other functional fiber membranes with hierarchical structures, which may find potential applications in adsorption, catalysis, filtration, and other water remediation fields.

■ AUTHOR INFORMATION

Corresponding Author
*Tel: 86-21-55664197. Fax: 86-21-65640293. E-mail: txliu@fudan.edu.cn.

Notes
The authors declare no competing financial interest.

■ ACKNOWLEDGMENTS

■ REFERENCES

(1) Chen, C.; Gunawan, P.; Xu, R. J. Mater. Chem. **2011**, 21, 1218−1225.

(2) Singh, S.; Barick, K. C.; Bahadur, D. J. Hazard. Mater. **2011**, 192, 1539−1547.

(3) Stein, A.; Wang, Z.; Fierke, M. A. Adv. Mater. **2009**, 21, 265−293.

(4) Zeng, Q.; Wu, D.; Zou, C.; Xu, F.; Fu, R.; Li, Z.; Liang, Y.; Su, D. Chem. Commun. **2010**, 46, 5927−5929.

(5) Yu, M.; Wang, H.; Zhou, X.; Yuan, P.; Yu, C. J. Am. Chem. Soc. **2007**, 129, 14576−14577.

(6) Zhuang, X.; Zhao, Q.; Wan, Y. J. Mater. Chem. **2010**, 20, 4715−4724.

(7) Gu, F. N.; Wei, F.; Yang, J. Y.; Lin, N.; Lin, W. G.; Wang, Y.; Zhu, J. H. Chem. Mater. **2010**, 22, 2442−2450.

(8) Studart, A. R.; Studer, J.; Xu, L.; Yoon, K.; Shum, H. C.; Weitz, D. A. Langmuir **2011**, 27, 955−964.

(9) Yuan, Q.; Yin, A.-X.; Luo, C.; Sun, L.-D.; Zhang, Y.-W.; Duan, W.-T.; Liu, H.-C.; Yan, C.-H. J. Am. Chem. Soc. **2008**, 130, 3465−3472.

(10) Cai, W.; Hu, Y.; Chen, J.; Zhang, G.; Xia, T. CrystEngComm **2012**, 14, 972−977.

(11) Zhao, Y.; Frost, R. L.; Martens, W. N.; Zhu, H. Y. Langmuir **2007**, 23, 9850−9859.

(12) Zhang, J.; Liu, S.; Lin, J.; Song, H.; Luo, J.; Elssfah, E. M.; Ammar, E.; Huang, Y.; Ding, X.; Gao, J.; Qi, S.; Tang, C. J. Phys. Chem. B **2006**, 110, 14249−14252.

(13) Bruhne, S.; Gottlieb, S.; Assmus, W.; Alig, E.; Schmidt, M. U. Cryst. Growth Des. **2008**, 8, 489−493.

(14) Cai, W.; Yu, J.; Jaroniec, M. J. Mater. Chem. **2010**, 20, 4587−4594.

(15) Hashmi, A. S. K.; Hutchings, G. J. Angew. Chem., Int. Ed. **2006**, 45, 7896−7936.

(16) Guan, Z.; Liu, L.; He, L.; Yang, S. J. Hazard. Mater. **2012**, 196, 270−277.

(17) Fenn, J. B.; Mann, M.; Meng, C. K.; Wong, S. F.; Whitehouse, C. M. Science **1989**, 246, 64−71.

(18) Yang, D.-J.; Kamienchick, I.; Youn, D. Y.; Rothschild, A.; Kim, I.-D. Adv. Funct. Mater. **2010**, 20, 4258−4264.

(19) Xiao, S.; Shen, M.; Guo, R.; Wang, S.; Shi, X. J. Phys. Chem. C **2009**, 113, 18062−18068.

(20) Zhang, M.; Shao, C.; Guo, Z.; Zhang, Z.; Mu, J.; Cao, T.; Liu, Y. ACS Appl. Mater. Interfaces **2011**, 3, 369−377.

(21) Zhang, X.; Shao, C.; Zhang, Z.; Li, J.; Zhang, P.; Zhang, M.; Mu, J.; Guo, Z.; Liang, P.; Liu, Y. ACS Appl. Mater. Interfaces **2012**, 4, 785−790.

(22) Fang, X.; Xiao, S.; Shen, M.; Guo, R.; Wang, S.; Shi, X. New J. Chem. **2011**, 35, 360−368.

(23) Lee, J. A.; Nam, Y. S.; Rutledge, G. C.; Hammond, P. T. Adv. Funct. Mater. **2010**, 20, 2424−2429.

(24) Fang, X.; Ma, H.; Xiao, S.; Shen, M.; Guo, R.; Cao, X.; Shi, X. J. Mater. Chem. **2011**, 21, 4493−4501.

(25) Huang, Y.; Ma, H.; Wang, S.; Shen, M.; Guo, R.; Cao, X.; Zhu, M.; Shi, X. ACS Appl. Mater. Interfaces **2012**, 4, 3054−3061.

(26) Xiao, S.; Wu, S.; Shen, M.; Guo, R.; Huang, Q.; Wang, S.; Shi, X. ACS Appl. Mater. Interfaces **2009**, 1, 2848−2855.

(27) Caruso, R. A.; Schattka, J. H.; Greiner, A. Adv. Mater. **2001**, 13, 1577−1579.

(28) Hyuk, I. J.; Jae, Y. S.; Hun, Y. C.; Rae, P. C. Nanotechnology **2012**, 23, 035604 (10 ppm).

(29) Wang, R. Y.; Guo, J.; Chen, D.; Miao, Y.-E.; Pan, J. S.; Tjiu, W. W.; Liu, T. X. J. Mater. Chem. **2011**, 21, 19375−19380.

(30) Zhou, Y.-T.; Nie, H.-L.; Branford-White, C.; He, Z.-Y.; Zhu, L.-M. J. Colloid Interface Sci. **2009**, 330, 29−37.

(31) Choi, S.-S.; Chu, B. Y.; Hwang, D. S.; Lee, S. G.; Park, W. H.; Park, J. K. Thin Solid Films **2005**, 477, 233−239.

(32) Zhang, G.; Kataphinan, W.; Teye-Mensah, R.; Katta, P.; Khatri, L.; Evans, E. A.; Chase, G. G.; Ramsier, R. D.; Reneker, D. H. Mater. Sci. Eng., B **2005**, 116, 353−358.

(33) Guo, M.; Ding, B.; Li, X.; Wang, X.; Yu, J.; Wang, M. J. Phys. Chem. C **2010**, 114, 916−921.

(34) Yu, C.; Dong, X.; Guo, L.; Li, J.; Qin, F.; Zhang, L.; Shi, J.; Yan, D. J. Phys. Chem. C **2008**, 112, 13378−13382.

(35) Zhao, Z.-G.; Nagai, N.; Kodaira, T.; Hukuta, Y.; Bando, K.; Takashima, H.; Mizukami, F. J. Mater. Chem. **2011**, 21, 14984−14989.

(36) Bao, N.; Li, Y.; Wei, Z.; Yin, G.; Niu, J. J. Phys. Chem. C **2011**, 115, 5708−5719.

(37) Zhao, Y.; He, S.; Wei, M.; Evans, D. G.; Duan, X. Chem. Commun. **2010**, 46, 3031−3033.

(38) Wu, R.; Qu, J.; Chen, Y. Water Res. **2005**, 39, 630−638.